

Having demonstrated dark incoherent solitons, we address several issues. First, from earlier calculations (19) and present experiments we find (within the parameters explored) that the fundamental dark incoherent soliton requires a transverse phase jump (discontinuity) at the center of the dark stripe. How exactly the phase jump survives throughout propagation is still unclear. Second, it is apparent that a different theoretical approach should be pursued to find the stationary dark incoherent soliton solutions and their properties. Such a theory should rely on the modal approach of (16), but incorporate radiation modes as well as multiple guided modes. Therefore, it seems that dark incoherent solitons, or, in a broader sense, self-trapped dark incoherent wavepackets, are fundamentally a new concept: they resemble neither coherent dark solitons nor incoherent bright solitons.

In conclusion, we have demonstrated self-trapping of dark incoherent light beams. Although we employed quasi-monochromatic "partially" spatially incoherent sources, our results suggest that "fully" (spatially and temporally) incoherent dark solitons can be generated using incoherent white-light source. Our results provide direct evidence that a self-trapped incoherent dark beam induces a waveguide that may be used to guide other coherent or incoherent beams. Yet, our observations leave several open questions. For example, how does this incoherent beam maintain the "phase memory" throughout propagation in spite of the random phase fluctuations? Furthermore, our calculations (16, 19) show that the statistics of an incoherent beam are affected by the process of self-trapping. In particular, the coherence length increases in a dark self-trapped beam (inside and close to the dark stripe). This means that dark incoherent solitons can be used for coherence control. It is yet an experimental challenge to actually observe this behavior. We therefore expect that incoherent solitons will bring about new fundamental ideas in nonlinear science. This is especially true because solitons are a universal phenomenon that appears in any nonlinear dispersive system in nature (25).

REFERENCES AND NOTES

- See review papers by Y. S. Kivshar [*IEEE J. Quantum Electron.* **28**, 250 (1993)] and by Y. S. Kivshar and B. Luther-Davies [*Phys. Rep.* **298**, 81 (1998)].
- G. A. Swartzlander, D. R. Andersen, J. J. Regan, H. Yin, A. E. Kaplan, *Phys. Rev. Lett.* **66**, 1583 (1991).
- G. R. Allan, S. R. Skinner, D. R. Andersen, A. L. Smirl, *Opt. Lett.* **16**, 156 (1991).
- G. Duree *et al.*, *Phys. Rev. Lett.* **74**, 1978 (1995).
- M. D. Iturbe-Castillo, J. J. Sanchez-Mondragon, S. I. Stepanov, M. B. Klein, B. A. Wechsler, *Opt. Comm.* **118**, 515 (1995).
- Z. Chen *et al.*, *Opt. Lett.* **21**, 629 (1996); Z. Chen, M. Segev, S. Singh, T. Coskun, D. N. Christodoulides, *J. Opt. Soc. Am. B* **14**, 1407 (1997).
- G. A. Swartzlander and C. T. Law, *Phys. Rev. Lett.* **69**, 2503 (1992).
- B. Luther-Davies, R. Powles, V. Tikhonenko, *Opt. Lett.* **19**, 1816 (1994).
- A. V. Mamaev, M. Saffman, A. A. Zozulya, *Phys. Rev. Lett.* **78**, 2108 (1997).
- Z. Chen, M. Segev, D. Wilson, R. E. Muller, P. D. Maker, *ibid.*, p. 2948.
- , *Opt. Lett.* **23**, 1751 (1997).
- M. Mitchell, Z. Chen, M. Shih, M. Segev, *Phys. Rev. Lett.* **77**, 490 (1996).
- M. Mitchell and M. Segev, *Nature* **387**, 880 (1997).
- Incoherent solitons were first suggested in plasma physics by A. Hasegawa [*Phys. Fluids* **18**, 77 (1975); **20**, 2155 (1977)], who employed a quasi-particle approach. By averaging over the dynamics of these quasi-particles, a Vlasov transport equation was obtained and solved. Later on, Hasegawa has suggested another technique that further approximates the quasi-particles as plane waves [*Opt. Lett.* **5**, 416 (1980)] and predicted incoherent temporal solitons in multimode optical fibers.
- D. N. Christodoulides, T. Coskun, M. Mitchell, M. Segev, *Phys. Rev. Lett.* **78**, 646 (1997). This coherent density approach is primarily useful to analyze dynamical propagation behavior of arbitrary incoherent beams.
- M. Mitchell, M. Segev, T. Coskun, D. N. Christodoulides, *Phys. Rev. Lett.* **79**, 4990 (1997). This paper provides a modal theory of incoherent bright solitons and finds the soliton solutions, their properties (shape, coherence function), and the range in parameter space that supports them.
- D. N. Christodoulides, T. Coskun, M. Mitchell, M. Segev, *Phys. Rev. Lett.* **80**, 2310 (1998). This paper shows that the coherent density approach and the modal theory developed in (16) are equivalent and complement each other in terms of providing direct information about both the stationary and the dynamic propagation behavior of incoherent bright solitons.
- A. W. Snyder and D. J. Mitchell, *Phys. Rev. Lett.* **80**, 1422 (1998). This work employs a geometrical optics approach for analyzing bright incoherent solitons in the extreme limit of beams that are much larger than their correlation distance.
- T. H. Coskun, D. N. Christodoulides, M. Mitchell, Z. Chen, M. Segev, *Opt. Lett.* **23**, 418 (1998).
- M. Segev, G. C. Valley, B. Crosignani, P. DiPorto, A. Yariv, *Phys. Rev. Lett.* **73**, 3211 (1994); D. N. Christodoulides and M. I. Carvalho, *J. Opt. Soc. Am. B* **12**, 1628 (1995); M. Segev, M. Shih, G. Valley, *ibid.* **13**, 706 (1996).
- The observation of steady-state self-focusing in biased photorefractive crystals was first reported by M. D. Iturbe-Castillo, P. A. Marquez-Aguilar, J. J. Sanchez-Mondragon, S. Stepanov, V. Vysloukh [*Appl. Phys. Lett.* **64**, 408 (1994)].
- The observation of photorefractive screening solitons was first made by M. Shih *et al.*, *Electron. Lett.* **31**, 826 (1995); *Opt. Lett.* **21**, 324 (1996).
- Self-bending of photorefractive screening solitons was first predicted by S. Singh and D. N. Christodoulides [*Opt. Comm.* **118**, 569 (1995)] and first observed with bright solitons in (22). Later on, it was shown [S. Singh, M. I. Carvalho, D. N. Christodoulides, *ibid.* **130**, 288 (1996)] that at large enough applied fields, the self-bending increases with the field.
- A. W. Snyder, L. Polodian, D. J. Mitchell, *Opt. Lett.* **17**, 789 (1992).
- "Solitons are a gift from God. Therefore it is a sin not to use them." A. Hasegawa, at a Colloquium at Princeton University, December 1997.
- Supported by the U.S. Army Research Office, the U.S. Air Force Office of Scientific Research, and NSF.

22 January 1998; accepted 11 March 1998

Ultrathin Films of a Polyelectrolyte with Layered Architecture

A. R. Esker, C. Mengel, G. Wegner*

Posttransfer modification of preformed Langmuir-Blodgett films of poly(*tert*-butyl methacrylate) and poly(*tert*-butyl acrylate) by gaseous hydrochloric acid yields films with layered architecture of poly(methacrylic acid) and poly(acrylic acid), respectively. X-ray reflectivity and infrared spectroscopy confirm monolayer by monolayer transfer of the source polymers and their transformation to acid multilayer assemblies with retention of low surface roughnesses. The incorporation of cross-linking groups into the system offers the possibility for further chemical modification to produce ultrathin films of model networks desirable for bioadsorption studies and as hydrophilic spacing layers for tethered membranes.

The Langmuir-Blodgett (LB) technique offers the possibility to fabricate highly ordered films with monolayer by monolayer control of thickness and low surface roughnesses (1). In addition, nearly ideal model surfaces are obtained, the properties of which are controlled by the chemical structure of the last layer in the transfer process. These properties are desirable for a number

of applications such as model surfaces for protein adsorption, modified substrates for supported membranes, and microelectronic and optical devices (2–4). Unfortunately, not all molecules, such as water-soluble polymers, can be processed into single-component multilayers by this technique. Appropriate materials must have the proper balance between hydrophilic and hydrophobic properties and also between rigid (shape-persistent) and flexible moieties to facilitate the formation of a stable, liquid, crystalline-like monolayer phase at the air-water interface (4). This balance is neces-

Max-Planck-Institut für Polymerforschung, Ackermann Weg 10, D-55128 Mainz, Germany.

*To whom correspondence should be addressed. E-mail: wegner@mpip-mainz.mpg.de

sary to ensure that the film has suitable rheological properties for LB multilayer fabrication. Examples of materials suitable for the use of this technique include fatty acids, phospholipids, hairy rod polymers, and some polymers with long hydrophobic side chains (1–4). A more diverse set of materials such as nanoparticles, porphyrins, phthalocyanines, oligothiophenes, proteins, and many others form stable monolayers at the air-water interface (1, 2, 4). Some of these materials can be transferred to solid substrates as LB monolayers, sometimes even as multilayers, and many can be co-transferred with transferable molecules to produce composite LB multilayers. This idea has even been used to produce composite LB films containing ionically associated water-soluble polyelectrolytes and copolymers composed of soluble, ionizable, and LB-transferable monomers (5–7).

The molecules that we used in this study, poly(methacrylic acid) (PMAA) and poly(acrylic acid) (PAA), are too hydrophilic to form pure LB multilayers (Fig. 1, A to C). In order to obtain hydrophilic surfaces with high carboxylic acid densities desirable for models of superabsorbing polymer networks (8), for use in bioadsorption studies (9), and as precursors for subsequent chemical modification (7), a different approach was required. Posttransfer modification by wet, gas-

eous hydrochloric acid at room temperature was recently used to regenerate LB films of cellulose (10). We used a similar strategy here. If poly(*tert*-butyl methacrylate) (PtBMA) and poly(*tert*-butyl acrylate) (PtBA) are used as the precursor molecules, films of PMAA and PAA can be obtained through the elimination of gaseous isobutene under acidic hydrolysis conditions (Fig. 2). In contrast to the regeneration of cellulose hydroxyl groups (10), this process leads to the regeneration of carboxylic acid groups and hence a polyelectrolyte with different surface properties and chemical reactivity.

The first step is necessarily the formation of stable monolayers at the air-water interface (Fig. 2A). In the case of PtBMA, this behavior is already well known through monolayer studies of its isotherms, surface rheology, and dynamics (11, 12). For PtBA, isotherm studies also exist (11). For the samples studied here (13), the only significant difference between PtBMA and PtBA is an increase in the transition surface pressure for PtBA ($\Pi \approx 4 \text{ mN m}^{-1}$) between an expanded and a condensed surface film compared with PtBMA ($\Pi < 1 \text{ mN m}^{-1}$). This difference is presumably a consequence of the missing methyl groups on the PtBA polymer backbone, which leads to increased film hydrophilicity and an attendant increase in the amount of water adsorbed to the film. This increased adsorption causes greater disruption of water's structure in the expanded regime of the PtBA isotherm (lowering the

surface tension) and can also act as a plasticizer, making the film more flexible.

The second step (Fig. 2B), LB transfer of the materials, is related to the isotherm. PtBMA undergoes LB transfer (3). In this study, monodisperse three-arm PtBMA stars (Fig. 1C) were found to have isotherms similar to those of linear PtBMA of comparable molecular weight and to undergo quantitative LB transfer, as does PtBA (14). In both cases, the transfer proceeds by vertical Y-type deposition, in which one monolayer is transferred on each up and down stroke of the substrate. This behavior has been confirmed by x-ray reflectivity (15). In the reflectivity profiles for both PtBMA and PtBA (Fig. 3), the most significant difference is the presence of a well-defined Bragg peak for PtBA at a wave vector around $q \approx 0.35 \text{ \AA}^{-1}$, which confirms the $\approx 18 \text{ \AA}$ double-layer structure depicted in Fig. 2B. Bragg peaks are observed for PtBA samples of sufficient layers ($\geq \approx 30$) if the root-mean-square roughness of the substrate is sufficiently low ($\sigma_s < \approx 7 \text{ \AA}$). This behavior was not seen for PtBMA, which suggests that the methyl groups along the backbone alter the packing characteristics significantly. This interpretation is also supported by the relation between the film thickness, D , and the number of layers

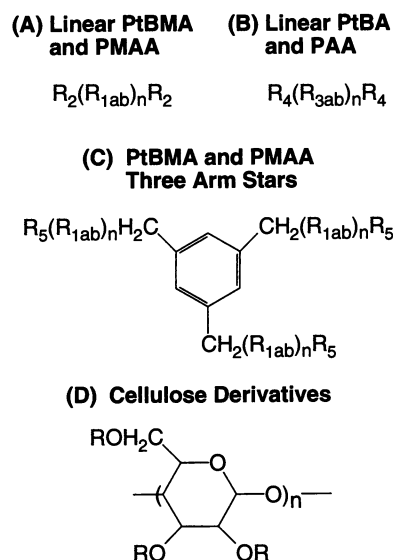


Fig. 1. Polymers used in this study. (A) Linear PtBMA and PMAA. (B) Linear PtBA and PAA. (C) PtBMA and PMAA three-arm stars. (D) Cellulose derivatives. $R_{1a} = -[CH_2C(CH_3)(COOC(CH_3)_3)]-$ (PtBMA); $R_{1b} = -[CH_2C(CH_3)(COOH)]-$ (PMAA); $R_2 = -CH_2(p-C_6H_4)CH=CH_2$ (styryl); $R_{3a} = -[CH_2CH(COOC(CH_3)_3)]-$ (PtBA); $R_{3b} = -[CH_2CH(COOH)]-$ (PAA); $R_4 = -CH_2CH=CH_2$ (allyl); $R_5 = -C(C_5H_{11})(C_6H_5)(C_{14}H_9)$ (pentyl, phenyl, anthryl); and R is a statistical distribution of $-H$ (hydroxyl), $-CH_2CH_2CH(CH_3)_2$ (isopentyl ether), and $-COCH=CHC_6H_5$ (cinnamate ester).

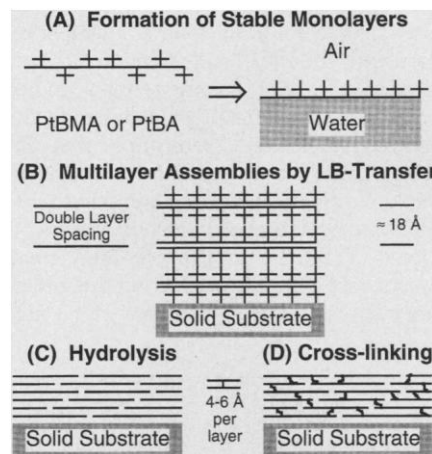


Fig. 2. Schematic depiction of the major steps in the LB approach for fabricating model networks in the form of ultrathin layers from PtBMA and PtBA. Confinement of the polymers at the air-water interface leads to a nearly two-dimensional conformation in which the *tert*-butyl groups (+) are preferentially oriented away from the aqueous subphase (A). In the case of PtBA, this leads to a double-layer structure as depicted in (B). Elimination of the *tert*-butyl groups (C) and photo-cross-linking (D) leads to PMAA or PAA films as polyelectrolytes. For this study, IPCC was added to the films at (A) to form network structures.

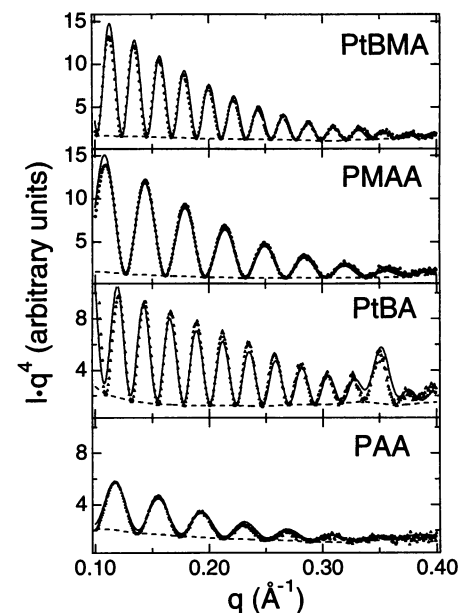


Fig. 3. Representative x-ray reflectivity profiles showing the scaled intensity ($I \cdot q^4$) as a function of the wave vector obtained from LB films (30 layers). The symbols and dashed lines represent the experimental data and background, respectively, and the solid lines represent the fitted curves according to the established procedure (15). The relevant surface parameters for the curves (electron density in per electron per cubic angstrom) and D , σ_p , and σ_s in angstroms) are as follows: PtBMA (0.33, 287, 5, 5); PMAA (0.34, 178, 5, 5); PtBA (0.30, 271, 4, 4); and PAA (0.36, 165, 6, 4).

obtained from fitting reflectivity profiles (Fig. 4). The linear relation confirms monolayer by monolayer transfer, with the slope providing the thickness of a single monolayer. For PtBMA, the thickness per layer and the transfer area can be used to calculate the film density, $\rho = 1.00 \text{ g cm}^{-3}$, a value that is in excellent agreement with the bulk value of $\rho = 1.02 \text{ g cm}^{-3}$ (16). In contrast, PtBA's calculated density, $\rho = 0.91 \text{ g cm}^{-3}$, is significantly lower than the bulk density of $\rho = 1.00 \text{ g cm}^{-3}$ (16). These values imply that PtBMA has similar packing at both the air-water interface and in the bulk. In contrast, the absence of the methyl group allows PtBA to significantly alter its conformation in such a way that all of the hydrophobic *tert*-butyl side groups at the air-water interface can be oriented away from the surface (Fig. 2). This is consistent with both the decreased density and the observed double-layer structure.

At this point, the scheme presented in Fig. 2 offers some flexibility. As presented, hydrolysis precedes cross-linking (Fig. 2C). In practice, these steps are interchangeable. For this study, hydrolysis has been the primary focus. Capitalizing on the ability to eliminate gaseous isobutene from *tert*-butyl esters, we subjected LB films of PtBMA and PtBA to 6-hour treatments with wet gaseous hydrochloric acid at 60°C. Reflectivity profiles (Fig. 3) show that the elimination of *tert*-butyl groups proceeds without significantly increasing the film's surface roughness, σ_p . Linear relations between the thickness of the PMAA and PAA films and the number of layers originally deposited (Fig. 4) suggest that, even though the double-layer structure is destroyed, the layered structure may not be lost. This would also be consistent with the prohibitive effect the high glass transition temperatures of the transferred and hydrolyzed species (16) would have on the molecular mobility re-

quired for changes in polymer conformation from two- to three-dimensional structures and the absence of significantly rougher surfaces or dewetting which would be expected to accompany such a process. From the transfer conditions and the new thicknesses, densities for PMAA and PAA films can be estimated as $\rho = 1.05$ and 1.14 g cm^{-3} , respectively. In addition to x-ray reflectivity, we used infrared spectroscopy to confirm the elimination of the *tert*-butyl groups and transformation to the desired acid monolayers (17). In the infrared spectrum for PMAA, changes in the carbonyl and C–O stretch along with the growth of a broad hydroxyl stretch are consistent with the hydrolysis of PtBMA and PMAA existing primarily as acid dimer (Fig. 5). From the thickness measurements, the elimination of the *tert*-butyl groups appears to be complete.

If we return to the scheme in Fig. 2, the next important step is the ability to form "network" structures. Feasibility studies with mixed films of isopentylcellulose cinnamate (IPCC) and linear α,ω -*p*-vinylbenzyl-functionalized PtBMA verified that this is possible (13). The cross-linking was photoinduced by 254-nm ultraviolet light (18) (Fig. 2D). In addition to the expected photoaddition, other reactions are possible. When molecules containing olefinic bonds are present, photoinduced cross-linking involving these moieties is observed. For mixtures of IPCC with noncross-linkable isopentyl cellulose (IPC), the thickness of cross-linked films after extraction of noncross-linkable material by chloroform follows a simple relation with the IPCC mole fraction, $D_{\text{final}} = x_{\text{IPCC}} \cdot D_{\text{initial}}$ (19). For the systems studied here, D_{final} is significantly smaller than the observed thicknesses, indicating that PtBMA is incorporated into insoluble network structures. Subsequent treatment with hydrochloric acid as above converts the incorporated PtBMA to PMAA. For small amounts of PtBMA, the effect on the surface roughness is small. However, for large

amounts of PtBMA, there are an insufficient number of cross-linking groups to form well-defined networks. Thus, significant amounts of PtBMA are also extracted from the film. For this system, the practical limit is about $\approx 60\%$ PtBMA, which gives films that are $\approx 70\%$ of the original thickness after chloroform extraction.

The well-defined films of PMAA and PAA that we have been prepared by post-transfer modification of PtBMA and PtBA precursor LB films are potential precursors for supramolecular chemistry at surfaces. Ongoing work is focusing on the incorporation of photo-cross-linkable groups into the precursor polymers and further chemical derivatization of these films. These studies will differ significantly from other studies on polyelectrolyte thin films that are made up of alternating layers of oppositely charged species through self-assembly processes (20). Polyelectrolyte films obtained from LB precursors offer subnanometer control of thickness (single monomer increments) and roughness and the possibility of locking in two-dimensional polymer conformations through cross-linking for a single chemical species without sacrificing any ionizable functional groups to intermolecular interactions.

In contrast, films generated from and held together by alternating layers of oppositely charged polyelectrolytes offer only nanoscale control of thickness (molecule versus monomer-thick layers) and require at least two unique chemical species (20). However, this later process does not require special equipment or have as many substrate restrictions as the LB technique and may be preferable when the greater order inherent in LB films is not required. Polyelectrolytes obtained from precursor LB films are also different from other thin film assemblies based on PAA such as grafted systems (21), complexation to LB films (6), and LB films of copolymers (7) for similar reasons. Moreover, the possibility of retaining the two-dimensional conformation of PMAA and PAA after hydrolysis by first

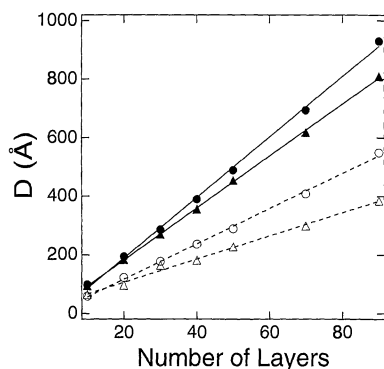


Fig. 4. The dependence of the film thickness on the number of layers for PtBMA (●), PtBA (▲), PMAA (○), and PAA (△). Thicknesses per layer obtained from the slopes with $\pm 95\%$ confidence intervals are 10.3 ± 0.5 , 8.9 ± 0.2 , 6.0 ± 0.3 , and $4.0 \pm 0.4 \text{ Å}$, respectively.

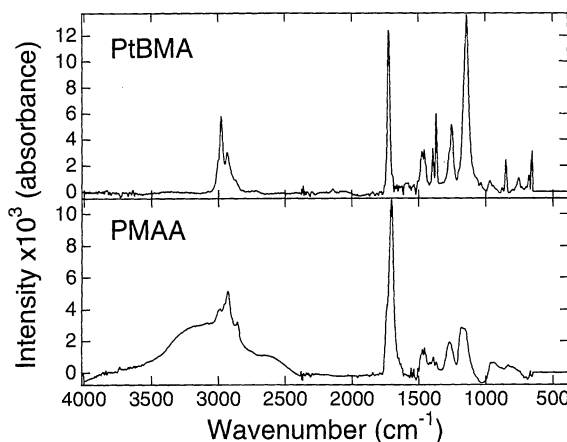


Fig. 5. IR spectra for LB films of PtBMA and PMAA. Hydrolysis of PtBMA leads to a shift in the carbonyl stretch from 1723 to 1700 cm^{-1} , attenuation of the C–O stretch at 1140 cm^{-1} , and the growth of a broad hydroxyl stretch at around 3400 cm^{-1} , consistent with the formation of the PMAA dimer.

cross-linking the material makes it possible to assemble composite structures that differ by as little as a single monolayer (one monomer thick). In addition to uses as models of superabsorbing polymer networks (8) and in bioadsorption studies (9), these materials should be ideal for the flexible hydrophilic spacing layers needed between supported bilayers and solid substrates for biologically relevant studies of the physical properties of membranes (22).

REFERENCES AND NOTES

1. M. C. Petty, *Langmuir-Blodgett Films: An Introduction* (Cambridge Univ. Press, Cambridge, 1996); G. Roberts, Ed., *Langmuir-Blodgett Films* (Plenum, New York, 1990).
2. A. Ulman, *An Introduction to Ultrathin Organic Films: From Langmuir-Blodgett to Self-Assembly* (Academic Press, Boston, 1991); J. D. Swalen, *J. Mol. Electron.* **2**, 155 (1986).
3. W. M. K. P. Wijekoon *et al.*, *J. Am. Chem. Soc.* **118**, 4480 (1996); T. L. Penner, H. R. Motschmann, N. J. Armstrong, M. C. Ezenyilimba, D. Williams, *Nature* **367**, 49 (1994); K. Clays, N. J. Armstrong, T. L. Penner, *J. Opt. Soc. Am. B* **10**, 886 (1993); K. Clays, N. J. Armstrong, M. C. Ezenyilimba, T. L. Penner, *Chem. Mater.* **5**, 1032 (1993).
4. G. Wegner, *Mol. Cryst. Liq. Cryst.* **235**, 1 (1993).
5. R. Rulken, G. Wegner, V. Enkelmann, M. Schulze, *Ber. Bunsenges. Phys. Chem.* **100**, 707 (1996).
6. M. Bardosova, R. H. Tredgold, Z. Ali-Adib, *Langmuir* **11**, 1273 (1995); A. Takahara *et al.*, *Macromolecules* **22**, 617 (1989).
7. M. Tamura and A. Sekiya, *Chem. Lett.* **1991**, 399 (1991).
8. K. S. Kazanskii and S. A. Dubrovskii, *Adv. Polym. Sci.* **104**, 97 (1992); R. Po, *Rev. Macromol. Chem. Phys.* **34**, 607 (1994).
9. A. Hartmann and S. Seeger, *Thin Solid Films* **245**, 206 (1994); H. Fukushima, H. Morgan, D. M. Taylor, *ibid.* **244**, 789 (1994); S. Seeger *et al.*, in *Synthetic Microstructures in Biological Research*, J. M. Schnur and M. Peckerar, Eds. (Plenum, New York, 1992), p. 586.
10. V. Buchholz *et al.*, *Langmuir* **13**, 3206 (1997); V. Buchholz, G. Wegner, S. Stemme, L. Ödberg, *Adv. Mater.* **8**, 399 (1996); M. Schaub, G. Wenz, G. Wegner, A. Stein, D. Klemm, *ibid.* **5**, 919 (1993).
11. J. E. Sutherland and M. L. Miller, *J. Polym. Sci. B* **7**, 871 (1969).
12. M. Sacchetti, H. Yu, G. Zografi, *Langmuir* **9**, 2168 (1993); S. Kim and H. Yu, *Progr. Colloid Polym. Sci.* **89**, 202 (1992); M. Kawaguchi, B. B. Sauer, H. Yu, *Macromolecules* **22**, 1735 (1989).
13. The three-arm PtBMA stars (bearing anthryl end groups), linear PtBMA (α, ω -p-vinylbenzyl-functionalized), and PtBA (α, ω -allyl-functionalized) (Fig. 1C) were prepared by anionic polymerization. The cellulose derivatives (IPCC and IPC) (Fig. 1D) were prepared and characterized according to the method of M. Schaub [thesis, University of Mainz, Mainz, Germany (1993)]. Gel permeation chromatography with poly(styrene)/divinylbenzene columns (SDV 500, PSS Inc.) with mesh sizes of 10^3 , 10^5 , and 10^6 Å were used to deduce poly(methyl methacrylate) [poly(styrene) for the celluloses] standard number-average molecular weights (M_n in kilograms per mole) and polydispersities (M_w/M_n) of PtBMA star (33.7, 1.04), linear PtBMA (25.8, 1.18), PtBA (28.8, 1.50), IPCC (89.2, 1.96), and IPC (114, 1.97). The functionality of the PtBMA (95%) and PtBA (85%) end groups was determined by a 300-MHz ^1H nuclear magnetic resonance spectroscopy (Bruker). The cellulose derivatives had degrees of substitution of IPCC (2.1 isopentyl, 0.3 cinnamate, and 0.6 hydroxyl) and IPC (2.8 isopentyl, 0.2 hydroxyl) based on elemental analysis.
14. Transfer ratios of 1.00 ± 0.05 onto Si substrates hydrophobized with ammonium fluoride (x-ray experiments) or 1,1,1,3,3,3-hexamethyldisilazane (infrared studies) were obtained for all of the samples under the following conditions (temperature in degrees centigrade, surface concentration in angstroms squared per monomer, surface pressure in millinewtons per meter): PtBMA star (20, 22.9, 12), linear PtBMA (8 and 20, 22.7, 15), PtBA (8, 26.3, 15), IPCC (8, 63.0, 15 and 18), and IPC (8, 67.8, 18).
15. The periodic fluctuations seen in Fig. 3 represent Kiessig fringes, which arise from the interference between x-rays reflected from the Si-polymer and polymer-air interfaces. Knowing the position of the maxima, one can obtain the thickness of the film [P. Tippmann-Krayer, H. Möhwald, Yu. M. L'vov, *Langmuir* **7**, 2298 (1991)]. A more detailed analysis obtained by directly fitting the experimental profiles with theoretical curves also yields the roughness of both the film and the substrate. For this study, we applied the latter technique using the methods and experimental set-up described in M. Schaub *et al.*, *Macromolecules* **28**, 1221 (1995).
16. D. W. van Krevelen and P. J. Hoftyzer, *Properties of Polymers: Their Estimation and Correlation with Chemical Structure* (Elsevier, Amsterdam, 1976).
17. IR spectroscopy was carried out on a Nicolet Magna 850 Fourier-transform with LB films (80 to 100 layers) deposited on Si hydrophobized with 1,1,1,3,3,3-hexamethyldisilazane.
18. S. Iida, M. Schaub, M. Schulze, G. Wegner, *Adv. Mater.* **5**, 564 (1993); P. L. Egerton, E. Pitts, A. Reiser, *Macromolecules* **14**, 95 (1981).
19. An easy and reliable test of whether a network forms is to take the cross-linked LB film and immerse it in a good solvent [M. Seufert, M. Schaub, G. Wenz, G. Wegner, *Angew. Chem. Int. Ed. Engl.* **34**, 340 (1995)]. When the film is not a network, the film is soluble and leaves the substrate.
20. G. Decher, *Science* **277**, 1232 (1997).
21. M. L. Bruening *et al.*, *Langmuir* **13**, 770 (1997); Y. Zhou, M. L. Bruening, Y. Liu, R. M. Crooks, D. E. Bergbreiter, *ibid.* **12**, 5519 (1996); Y. Zhou, M. L. Bruening, D. E. Bergbreiter, R. M. Crooks, M. Wells, *J. Am. Chem. Soc.* **118**, 3773 (1996).
22. H. Sigl *et al.*, *Eur. Biophys. J.* **25**, 249 (1997); E. Sackmann, *Science* **271**, 43 (1996).
23. Financial support was provided by the Stockhausen GmbH & Co. KG.

16 December 1997; accepted 12 March 1998

The Biochemical Basis of an All-or-None Cell Fate Switch in *Xenopus* Oocytes

James E. Ferrell Jr.* and Eric M. Machleder

Xenopus oocytes convert a continuously variable stimulus, the concentration of the maturation-inducing hormone progesterone, into an all-or-none biological response—oocyte maturation. Here evidence is presented that the all-or-none character of the response is generated by the mitogen-activated protein kinase (MAPK) cascade. Analysis of individual oocytes showed that the response of MAPK to progesterone or Mos was equivalent to that of a cooperative enzyme with a Hill coefficient of at least 35, more than 10 times the Hill coefficient for the binding of oxygen to hemoglobin. The response can be accounted for by the intrinsic ultrasensitivity of the oocyte's MAPK cascade and a positive feedback loop in which the cascade is embedded. These findings provide a biochemical rationale for the all-or-none character of this cell fate switch.

Fully grown *Xenopus laevis* oocytes are arrested in a state that resembles the G_2 phase of the cell division cycle with inactive cyclin-dependent kinase Cdc2 and an intact germinal vesicle. Exposure to the hormone progesterone induces oocytes to undergo maturation, during which they activate Cdc2, undergo germinal vesicle breakdown, complete the first meiotic division, and finally arrest in metaphase of meiosis 2 (1). Oocyte maturation is an example of a true cell fate switch; oocytes can reside in either the G_2 arrest or the metaphase arrest state for extended periods of time, but can be in intermediate states only transiently.

Progesterone-induced maturation is thought to be triggered by activation of a cascade of protein kinases—Mos, Mek-1, and p42 or Erk2 MAP kinase (MAPK). Progesterone causes the accumulation of

Mos, which phosphorylates and activates Mek-1. Active Mek-1 in turn phosphorylates and activates p42 MAPK, which brings about activation of the Cdc2–cyclin B complex. Interfering with the accumulation of Mos (2) or the activation of Mek-1 (3) or p42 MAPK (4) inhibits progesterone-induced activation of Cdc2 and maturation, and microinjection of nondegradable Mos (5), constitutively active Mek-1 (4, 6), or thiophosphorylated p42 MAPK (7) brings about Cdc2 activation and maturation in the absence of progesterone. At some point in this chain of events, a continuously variable stimulus—the progesterone concentration—is converted into an all-or-none biological response.

Studies of the steady-state responses of the MAPK cascade in *Xenopus* oocyte extracts indicate that the cascade might contribute to the all-or-none character of oocyte maturation. In extracts, the response of MAPK to recombinant malE-Mos (a maltose-binding protein Mos fusion protein) is highly ultrasensitive (8), meaning it resem-

Department of Molecular Pharmacology, Stanford University School of Medicine, Stanford, CA 94305–5332, USA.

*To whom correspondence should be addressed. E-mail: ferrell@cmgm.stanford.edu